

Synthesis and Characterization of Low-Spin and Cation Radical Complexes of Ruthenium(III) of a Tridentate Pyridine Bis-Amide Ligand

Akhilesh Kumar Singh, V. Balamurugan, and Rabindranath Mukherjee*

Department of Chemistry, Indian Institute of Technology, Kanpur 208 016, India

Received April 2, 2003

Using a tridentate bis-amide ligand 2,6-bis(*N*-phenylcarbamoyl)pyridine (H_2L), in its deprotonated form, a new mononuclear ruthenium(III) complex $[Et_4N][RuL_2] \cdot H_2O$ (**1**) has been synthesized. Structural analysis reveals that the RuN_6 coordination comprises four deprotonated amide-N species in the equatorial plane and two pyridine-N donors in the axial positions, imparting a tetragonally compressed octahedron around Ru. To the best of our knowledge, this is the first time that a ruthenium(III) complex coordinated solely by two tridentate deprotonated peptide ligands has been synthesized and structurally characterized. When examined by cyclic voltammetry, complex **1** displays in MeCN/ CH_2Cl_2 solution three chemically/electrochemically reversible redox processes: a metal-centered reductive $Ru^{III}-Ru^{II}$ couple ($E_{1/2} = -0.84/-0.89$ V vs SCE) and two ligand-centered oxidative responses ($E_{1/2} = 0.59/0.60$ and $1.05/1.05$ V vs SCE). Isolation of a dark blue one-electron oxidized counterpart of **1**, $[RuL_2] \cdot H_2O$ (**2**), has also been readily achieved. The complexes have been characterized by analytical, solution electrical conductivity, IR, electronic absorption and EPR spectroscopy, and temperature-dependent magnetic susceptibility measurements. For complex **1**, a weak and broad transition within the t_{2g} level has been identified at ~ 1400 nm and supported by EPR spectral analysis ($S = 1/2$). Temperature-dependent magnetic susceptibility data provide unambiguous evidence that in **2** strong antiferromagnetic coupling of the $S = 1/2$ ruthenium atom with the $S = 1/2$ ligand π -cation radical leads to an effectively $S = 0$ ground state (1H NMR spectra in $CDCl_3$ solution).

Introduction

There has been a growing interest in the development of coordination chemistry of deprotonated peptide ligands derived from 2,6-pyridinedicarboxylic acid toward transition metal ions.^{1–5} Recently, we⁶ and others⁷ reported isolation

of the one-electron oxidized form of six-coordinate low-spin iron(III) complexes of type $[(bpb/Me_6bpb)Fe(CN)_2]^- [H_2bpb = 1,2-bis(pyridine-2-carboxamido)benzene; H_2Me_6bpb = 1,2-bis(3,5-dimethylpyridine-2-carboxamido)-4,5-dimethylbenzene]$. For such oxidized complexes, strong intramolecular antiferromagnetic coupling [$-2J \geq 450$ cm^{-1} ; singlet–triplet energy gap is expressed in terms of $2J$] between the metal unpaired d electron ($S = 1/2$) and the unpaired electron of ligand π -cation radical ($S = 1/2$), yielding an effectively $S = 0$ ground state for the iron(III) complex, was observed. Che et al. reported that low-spin iron(III) complexes of type $[Fe(bpc)(L)_2][ClO_4]$ [$H_2bpc = 1,2-bis(pyridine-2-carboxamido)-4,5-dichlorobenzene$, $L = Bu_3P$, Im, 1-MeIm, $tBu(py)$] exhibit well-behaved one-electron ligand-centered oxidation processes.^{8a} They observed similar ligand-centered oxidation processes with Co(III),^{8b} Rh(III),^{8c} and Ir(III)^{8c} complexes

* To whom correspondence should be addressed. E-mail: rnm@iitk.ac.in.

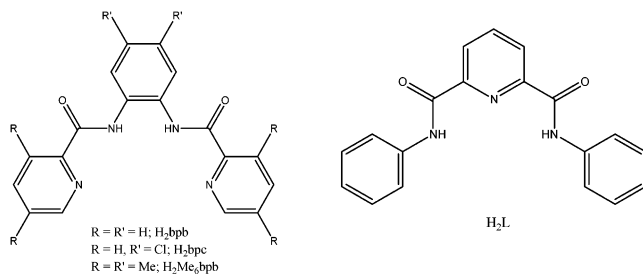
- (1) Marlin, D. S.; Mascharak, P. K. *Chem. Soc. Rev.* **2000**, 29, 69.
- (2) (a) Chavez, F. A.; Olmstead, M. M.; Mascharak, P. K. *Inorg. Chem.* **1996**, 35, 1410. (b) Chavez, F. A.; Olmstead, M. M.; Mascharak, P. K. *Inorg. Chem.* **1997**, 36, 6323. (c) Marlin, D. S.; Olmstead, M. M.; Mascharak, P. K. *Inorg. Chem.* **1999**, 38, 3258. (d) Noveron, J. C.; Olmstead, M. M.; Mascharak, P. K. *J. Am. Chem. Soc.* **1999**, 121, 3553. (e) Marlin, D. S.; Olmstead, M. M.; Mascharak, P. K. *Inorg. Chim. Acta* **2000**, 297, 106. (f) Marlin, D. S.; Olmstead, M. M.; Mascharak, P. K. *J. Mol. Struct.* **2000**, 554, 211. (g) Noveron, J. C.; Olmstead, M. M.; Mascharak, P. K. *J. Am. Chem. Soc.* **2001**, 123, 3247. (h) Marlin, D. S.; Olmstead, M. M.; Mascharak, P. K. *Inorg. Chem.* **2001**, 40, 7003.
- (3) (a) Ray, M.; Ghosh, D.; Shirin, Z.; Mukherjee, R. *Inorg. Chem.* **1997**, 36, 3568. (b) Patra, A. K.; Mukherjee, R. *Inorg. Chem.* **1999**, 38, 1388.
- (4) (a) Redmore, S. M.; Rickard, C. E. F.; Webb, S. J.; Wright, L. J. *Inorg. Chem.* **1997**, 36, 4743. (b) Yano, T.; Tanaka, R.; Nishioka, T.; Kinoshita, I.; Isobe, K.; Wright, L. J.; Collins, T. J. *Chem. Commun.* **2002**, 1396.
- (5) Kawamoto, T.; Hammes, B. S.; Ostrander, R.; Rheingold, A. L.; Borovik, A. S. *Inorg. Chem.* **1998**, 37, 3424.

- (6) (a) Ray, M.; Mukherjee, R.; Richardson, J. F.; Buchanan, R. M. *J. Chem. Soc., Dalton Trans.* **1993**, 2451 and references therein. (b) Patra, A. K.; Ray, M.; Mukherjee, R. *Inorg. Chem.* **2000**, 39, 652 and references therein.
- (7) Dutta, S. K.; Beckmann, U.; Bill, E.; Weyhermüller, T.; Wieghardt, K. *Inorg. Chem.* **2000**, 39, 3355.

of bpb(2-) and bpc(2-). But in either case, the oxidized products were not isolated, and their full characterization was not attempted.⁸

As a part of this program, we have developed the coordination chemistry of the tridentate dianion of 2,6-bis-(*N*-phenylcarbamoyl)pyridine (H₂L), and in the process, a number of complexes of the type [ML₂]^{z-} [M = Fe(III) and Co(III) (z = 1-); Ni(II) (z = 2-); Ni(IV) (z = 0)] have been synthesized and characterized by X-ray crystallography.³ Each complex contains two meridionally coordinated tridentate ligands to impart a tetragonally compressed octahedral geometry about the metal ion. It is worth mentioning here that the one-electron oxidation processes observed for [FeL₂]⁻ and [CoL₂]⁻ were arbitrarily assigned as ligand-centered.^{3a}

Collins et al. have shown that redox-inert macrocyclic tetraamido-*N* ligands are capable of stabilizing unusual non-oxo high-valent transition metal ions such as cobalt(IV) and iron(IV).⁹ They also demonstrated that such a macrocyclic ligand is noninnocent and structurally characterized a ligand π -cation radical complex of Co(III).¹⁰ Therefore, we felt that, by using a bis-ligand complex of ruthenium(III) supported by ligand L(2-), which interestingly provides nonmacrocyclic tetraamido-*N* coordination in the equatorial plane, it might be possible to generate and characterize [Ru^{IV}L₂] species. This hope was fueled by the added expectation that, for ruthenium, the generation/stabilization of the non-oxo ruthenium(IV) state would be facilitated. Our approach to this problem has been to work out a synthetic method to isolate a bis-ligand complex of ruthenium(III) that would allow the oxidized species to be isolated in the analytically pure form and to assign the correct formulation of such species. In the present work, we have studied the ruthenium chemistry with tridentate ligand H₂L, in its deprotonated form. Here, we report the isolation and characterization of the ruthenium(III) complex [Et₄N][RuL₂]·H₂O (**1**), including X-ray crystallography, and to firmly establish whether L(2-) is noninnocent, we prepared the one-electron oxidized complex [RuL₂]^{·-}·H₂O (**2**) and characterized it to a reasonable level of confidence.



Experimental Section

Materials and Reagents. All reagents were obtained from commercial sources and used as received. Solvents were dried/purified as reported previously. The ligand 2,6-bis(*N*-phenylcar-

bamoyl)pyridine and tetra-*n*-butylammonium perchlorate (TBAP) were prepared as before.^{3,11} [Ru(DMSO)₄Cl₂] was prepared following a reported procedure.¹²

Synthesis of Metal Complexes. (a) [Et₄N][RuL₂]·H₂O (1**).** The ligand H₂L (0.1 g, 0.315 mmol) was dissolved in dinitrogen-flushed *N,N'*-dimethylformamide (DMF) (15 mL), and to it was added solid NaH (0.015 g, 0.628 mmol), resulting in a light yellow solution. To it was added solid [Ru(DMSO)₄Cl₂] (0.076 g, 0.157 mmol) under dinitrogen atmosphere. The resulting solution was stirred for 10 min and refluxed for 6 h during which a color change to dark red was observed. To this was added solid [Et₄N]Cl·xH₂O (0.052 g, 0.314 mmol), and stirring was continued for 10 h. Removal of the solvent was followed by addition of MeCN (5 mL) and filtration. Slow evaporation afforded crystalline reddish-brown precipitate, which was filtered and washed with 5 mL of MeCN–Et₂O (1:5 v/v). The solid thus collected was dried in air (yield: 80 mg, ~58%).

Characterization. Anal. Calcd for C₄₆H₄₈N₇O₅Ru: C, 62.79; H, 5.46; N, 11.15. Found: C, 63.00; H, 5.50; N, 11.10. Conductivity (MeCN, ~1 mM solution at 298 K): $\Lambda_M = 125 \Omega^{-1} \text{ cm}^2 \text{ mol}^{-1}$ (expected range¹³ for 1:1 electrolyte: 120–160 $\Omega^{-1} \text{ cm}^2 \text{ mol}^{-1}$). Absorption spectrum [λ_{max} , nm (ϵ , M⁻¹ cm⁻¹): (in MeCN) 250 sh (27 700), 300 sh (13 500), 383 (11 200), 440 sh (8300), 1410 (270); (in CH₂Cl₂) 254 sh (28 050), 304 sh (13 450), 388 (11 400), 440 sh (8820).

(b) [RuL₂]^{·-}·H₂O (2**).** To a magnetically stirred solution of [Et₄N][RuL₂]·H₂O (**1**) (0.080 g, 0.09 mmol) in MeCN (3 mL) was added a solution of (NH₄)₂Ce(NO₃)₆ (0.060 g, 0.109 mmol) in MeCN (3 mL) dropwise. The dark blue compound that precipitated out was collected by filtration and washed with MeCN. The solid thus obtained was dried in vacuo (yield: 55 mg, ~83%).

Characterization. Anal. Calcd for C₃₈H₂₈N₆O₅Ru: C, 60.87; H, 3.74; N, 11.21. Found: C, 60.94; H, 3.80; N, 11.20. Conductivity (DMF, ~1 mM solution at 298 K): $\Lambda_M = 16 \Omega \text{ cm}^2 \text{ mol}^{-1}$ (expected range¹³ for 1:1 electrolyte: 65–90 $\Omega^{-1} \text{ cm}^2 \text{ mol}^{-1}$). Absorption spectrum [λ_{max} , nm (ϵ , M⁻¹ cm⁻¹): (in CH₂Cl₂) 303 (16 000), 360 sh (11 520), 658 (11 650). ¹H NMR (400 MHz, CDCl₃): δ 7.814 (2H, d, py-3,5-H), 7.655 (1H, t, py-4-H), 7.057 (3H, m, aromatic-3,4,5-H), 6.617 (2H, d, aromatic-2,6-H), 1.581 (s, H₂O).

Physical Measurements. Elemental analyses were obtained at the Department of Chemistry, Indian Institute of Technology Kanpur, India. Conductivity measurements were done with an Elico type CM-82T conductivity bridge (Hyderabad, India). Spectroscopic measurements were made using the following instruments: IR (KBr, 4000–600 cm⁻¹), Bruker Vector 22; electronic, Perkin-Elmer Lambda 2; X-band EPR, Varian 109 C (fitted with a quartz dewar for measurements at liquid-dinitrogen temperature), the spectra were calibrated with diphenylpicrylhydrazyl, DPPH ($g = 2.0037$).

Magnetic Measurements. Temperature-dependent magnetic susceptibility measurements on solid samples of **1** and **2** were done

- (9) (a) Anson, F. C.; Collins, T. J.; Coots, R. J.; Gipson, S. L.; Richmond, T. G. *J. Am. Chem. Soc.* **1984**, *106*, 5037. (b) Collins, T. J.; Kostka, K. L.; Münck, E.; Uffelman, E. S. *J. Am. Chem. Soc.* **1990**, *112*, 5637. (c) Collins, T. J.; Fox, B. G.; Hu, Z. G.; Kostka, K. L.; Münck, E.; Rickard, C. E. F.; Wright, L. J. *J. Am. Chem. Soc.* **1992**, *114*, 8724. (d) Kostka, K. L.; Fox, B. G.; Hendrich, M. P.; Collins, T. J.; Rickard, C. E. F.; Wright, L. J.; Münck, E. *J. Am. Chem. Soc.* **1993**, *115*, 6746. (10) Collins, T. J.; Powell, R. D.; Slebodnick, C.; Uffelman, E. S. *J. Am. Chem. Soc.* **1991**, *113*, 8419. (11) (a) Ray, M.; Mukerjee, S.; Mukherjee, R. *J. Chem. Soc., Dalton Trans.* **1990**, 3635. (b) Gupta, N.; Mukerjee, S.; Mahapatra, S.; Ray, M.; Mukherjee, R. *Inorg. Chem.* **1992**, *31*, 139. (12) Evans, I. P.; Spencer, A.; Wilkinson, G. *J. Chem. Soc., Dalton Trans.* **1973**, 204. (13) Geary, W. J. *Coord. Chem. Rev.* **1971**, *7*, 81.

- (8) (a) Che, C.-M.; Leung, W.-H.; Li, C.-K.; Cheng, H.-Y.; Peng, S.-M. *Inorg. Chim. Acta* **1992**, *196*, 43. (b) Mak, S.-T.; Wong, W.-T.; Yam, V. W.-W.; Lai, T.-F.; Che, C.-M. *J. Chem. Soc., Dalton Trans.* **1991**, 1915. (c) Mak, S.-T.; Yam, V. W.-W.; Che, C. M.; Mak, T. C. W. *J. Chem. Soc., Dalton Trans.* **1990**, 2555.

in the ranges $81 < T < 300$ K and $54 < T < 300$ K, respectively, using a locally built Faraday balance. The setup⁶ consists of an electromagnet with constant-gradient pole caps (Polytronic Corporation, Mumbai, India), Sartorius balance M-25-D/S (Göttingen, Germany), a closed cycle refrigerator, and a Lake Shore temperature controller (Cryo Industries, USA). All measurements were made at a fixed main field strength of ~ 6 kG. The calibration of the system and details of measurements are already reported in the literature.³

Solution-state magnetic susceptibilities were obtained by the NMR technique of Evans¹⁴ in MeCN with a PMX-60 JEOL (60 MHz) NMR spectrometer. Corrections underlying diamagnetism were applied with use of appropriate constants.¹⁵

Electrochemical Measurements. Cyclic voltammetric experiments were performed at 298 K by using a PAR model 370 electrochemistry system consisting of M-174A polarographic analyzer, M-175 universal programmer, and RE 0074 X-Y recorder. The cell contained a Beckman (M 39273) platinum-inlay working electrode, a Pt wire auxiliary electrode, and a saturated calomel electrode (SCE) as reference electrode. Details of the cell configuration are as described before.¹¹ For coulometry, a platinum-wire-gauze electrode was used as the working electrode. The solutions were ~ 1.0 mM in complex and 0.2 M in supporting electrolyte, TBAP.

Crystal Structure Determination. A reddish brown needle-shaped crystal of $[\text{Et}_4\text{N}][\text{RuL}_2]\cdot\text{H}_2\text{O}$ (**1**) (dimensions: $0.3 \times 0.2 \times 0.2$ mm³) was used for data collection. Diffracted intensities were collected on an Enraf Nonius CAD-4-Mach four-circle diffractometer using graphite-monochromated Mo K α radiation. Intensity data were corrected for Lorentz polarization effects; analytical absorption corrections were also applied. The structure was solved by SHELXS-86 (Patterson heavy atom method), expanded by Fourier-difference syntheses, and refined with the SHELXL97 package incorporated in WINGX 1.64 crystallographic collective package.¹⁶ The linear absorption coefficients, neutral atom scattering factors for the atoms, and anomalous dispersion corrections for non-hydrogen atoms were taken from ref 17. The positions of the hydrogen atoms were calculated assuming ideal geometries, but not refined. All non-hydrogen atoms were refined with anisotropic thermal parameters by full-matrix least-squares procedure on F^2 . We could not locate hydrogen atoms of the Et_4N^+ cation and water molecule from the electron density map. In fact, for this complex some disorder was observed with the Et_4N^+ cation. Two positions were identified as possible methylene carbon atoms, and they were refined with a site occupation factor of 0.5/0.5 and 0.6/0.4. The terminal methyl carbon sites C(20) and C(23) showed large displacement parameters indicating some degree of disorder but could not be resolved. An unassigned peak (2.471 \AA^3) was found near Ru atom at a distance of 0.949 Å, which may be due to the poor quality of crystal chosen for data collection. Pertinent crystallographic parameters are summarized in Table 1.

Results and Discussion

Synthesis. The synthesis of the ruthenium(III) compound $[\text{Et}_4\text{N}][\text{RuL}_2]\cdot\text{H}_2\text{O}$ (**1**) involved initial anaerobic reaction of

Table 1. Data Collection and Structure Refinement Parameters for $[\text{Et}_4\text{N}][\text{RuL}_2]\cdot\text{H}_2\text{O}$ (**1**)

param	1
chem formula	C ₄₆ H ₄₈ N ₇ O ₃ Ru
fw	879.98
temp/K	298
$\lambda/\text{\AA}$	0.710 73
cryst syst	monoclinic
cryst size/mm \times mm \times mm	$0.3 \times 0.2 \times 0.2$
space group	C2/c
$a/\text{\AA}$	9.809(7)
$b/\text{\AA}$	22.876(5)
$c/\text{\AA}$	19.734(2)
α/deg	90.0
β/deg	103.67(4)
γ/deg	90.0
$V/\text{\AA}^3$	4302(3)
Z	4
μ/mm^{-1}	0.418
no. reflns collected	3009
no. indep reflns	2814 ($R_{\text{int}} = 0.0180$)
GOF on F^2	1.301
final R indices [$I > 2\sigma(I)$]	R1 = 0.0945 wR2 = 0.2663
R indices (all data)	R1 = 0.1151 wR2 = 0.2900

Na_2L with $[\text{Ru}(\text{DMSO})_4\text{Cl}_2]$ in MeCN at 298 K followed by reflux at ~ 325 K forming a reddish-brown solution. Addition of $[\text{Et}_4\text{N}]\text{Cl}\cdot x\text{H}_2\text{O}$ and usual workup afforded reddish-brown air-stable crystals. Clean one-electron chemical oxidation of **1** in MeCN solution by $(\text{NH}_4)_2\text{Ce}(\text{NO}_3)_6$ generates a deep blue solution, which on usual workup led to the isolation of the product as a microcrystalline moisture sensitive blue solid, $[\text{RuL}_2]\cdot\text{H}_2\text{O}$ (**2**). Therefore, all manipulations with **2** were performed in dry atmosphere. Unfortunately, all attempts to grow single crystals of **2** for structural analysis failed so far.

The absence of $\nu(\text{N-H})$ in the IR spectra of these complexes indicates that the ligands are coordinated in the deprotonated form.¹⁸ A strong split band at 1602 and 1573 cm^{-1} in the spectrum of **1** is assigned to a C–O stretching frequency of $\nu(\text{amide I})$ vibration; in the spectrum of **2**, two bands at 1650 and 1629 cm^{-1} (Figure S1, Supporting Information) indicate an increase in the C–O bond strength that we associate with the different oxidation levels of L(2–) ligands in blue oxidized complex **2** (vide infra). We are convinced that this behavior is diagnostic of ligand oxidation (vide infra).^{6,7,10} A similar shift in the C–O stretching frequencies has been observed for low-spin Fe(III) and low-spin Fe(III) cation-radical complexes, recently reported from this laboratory.⁶ In MeCN solution, while complex **1** behaves as a 1:1 electrolyte, complex **2** is nonconducting, as expected.¹³ Elemental analyses, IR, and solution electrical conductivity data are in good agreement with the described formulations.

Description of the Structure of $[\text{Et}_4\text{N}][\text{RuL}_2]\cdot\text{H}_2\text{O}$ (1**).** A view of the metal environment in the anion of **1** is presented in Figure 1. The Ru atom sits on an imposed C_2 axis and is coordinated by four deprotonated amide nitrogens in the equatorial plane [N(1) and N(3) and their symmetry related] and two pyridyl nitrogens [N(2) and its symmetry

(14) Evans, D. F. *J. Chem. Soc.* **1959**, 2003.

(15) O'Connor, C. J. *Prog. Inorg. Chem.* **1992**, 32, 233.

(16) Farrugia, L. J. *WINGX version 1.64, An Integrated System of Windows Programs for the Solution, Refinement and Analysis of Single-Crystal X-ray Diffraction Data*; Department of Chemistry, University of Glasgow: Glasgow, 2003.

(17) *International Tables for X-ray Crystallography*; Kynoch Press: Birmingham, England, 1974; Vol. IV.

(18) Chapman, R. L.; Vagg, R. S. *Inorg. Chim. Acta* **1979**, 33, 227.

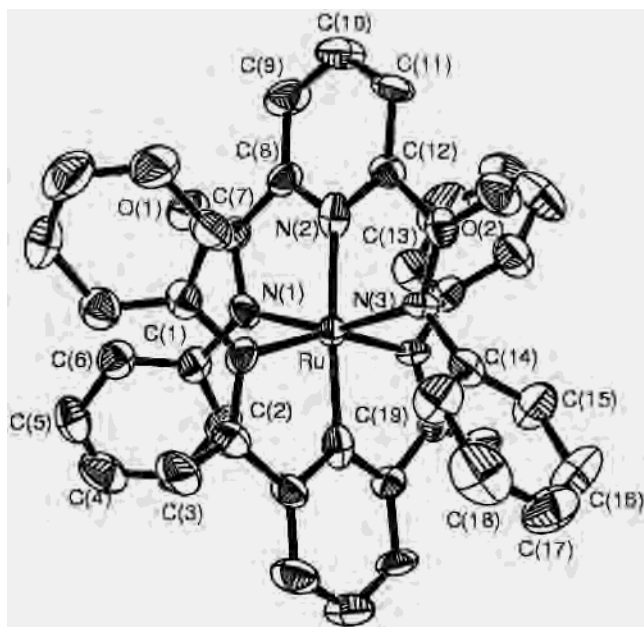


Figure 1. View of the structure of $[\text{RuL}_2]^-$ in the crystal of its Et_4N^+ salt, $[\text{Et}_4\text{N}][\text{RuL}_2]\cdot\text{H}_2\text{O}$ (**1**). Hydrogen atoms are omitted for clarity. Unlabeled atoms are related to labeled atoms by the crystallographic 2-fold axis.

Table 2. Selected Bond Lengths (Å) and Angles (deg) in the Anionic Part of $[\text{Et}_4\text{N}][\text{RuL}_2]\cdot\text{H}_2\text{O}$ (**1**)

Ru–N(1)	2.066(7)
Ru–N(2)	1.945(9)
Ru–N(3)	2.041(7)
N(1)–Ru–N(2)	79.5(3)
N(1)–Ru–N(3)	103.6(3)
N(2)–Ru–N(3)	158.3(3)
N(1)–Ru–N(3')	93.4(3)
N(2)–Ru–N(3')	78.9(3)
N(2)–Ru–N(3')	98.1(3)
N(1)–Ru–N(1')	89.4(3)
N(2)–Ru–N(2')	175.7(3)
N(3)–Ru–N(3')	91.9(3)

related] in the axial positions. The dihedral angle between the coordinating planes $\text{N}(1)\text{--Ru--N}(2)$ and $\text{N}(2)\text{--Ru--N}(3)$ is $\sim 178^\circ$, revealing meridional coordination of $\text{L}(2-)$, as that observed with its $\text{Fe}(\text{III})$, $\text{Co}(\text{III})$, $\text{Ni}(\text{II})$, and $\text{Ni}(\text{IV})$ analogues.³ The geometry of the RuN_6 coordination polyhedra is appreciably compressed octahedral (Table 2), as before.³ Significant deviation from 90° of the bond angles involving the chelation is observed (Table 2), presumably due to formation of five-membered chelate rings with extended conjugation, as observed for the bis-chelates reported previously.³ Further evidence of strain in the chelate rings arises from the following observation. Although in each ligand the two N-phenyl rings and the pyridine ring are planar, the two phenyl rings, however, make an angle of $\sim 80^\circ$, and they make angles of $\sim 60^\circ$ and $\sim 90^\circ$ with the central pyridine ring.

A few comments on metal–ligand bond distances are in order. The Ru--N_{py} bond distance of 1.945 Å in **1** is appreciably shorter than that observed for ruthenium(III) complexes of deprotonated pyridine amide ligand systems. For example, the Ru--N_{py} distances in $\text{cis-}[\text{Ru}(\text{pb})(\text{bpy})\text{Cl}_2]$ [$\text{Hpb} = 2\text{-(N-(4-nitro-phenylcarbamoyl)pyridine)}$]¹⁹ and in

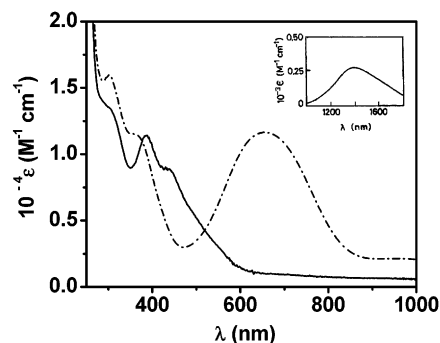


Figure 2. UV–vis spectra (in CH_2Cl_2) of $[\text{Et}_4\text{N}][\text{RuL}_2]\cdot\text{H}_2\text{O}$ (**1**) (—) and $[\text{RuL}_2]\cdot\text{H}_2\text{O}$ (**2**) (⋯). The low-energy band of $[\text{Et}_4\text{N}][\text{RuL}_2]\cdot\text{H}_2\text{O}$ (**1**) (in MeCN) is shown as an inset.

$[\text{Ru}(\text{bbpc})(\text{PPh}_3)\text{Cl}]$ [$\text{H}_2\text{bbpc} = 1,2\text{-bis(4-tert-butylpyridine-2-carboxamido)-4,5-dichlorobenzene}$]²⁰ are 2.055 and 2.088 Å, respectively. The $\text{Ru--N}_{\text{amide}}$ distance (2.054 Å) is appreciably longer than that found in above-mentioned complexes $\text{cis-}[\text{Ru}(\text{pb})(\text{bpy})\text{Cl}_2]$, 2.01 Å, and $[\text{Ru}(\text{bbpc})(\text{PPh}_3)\text{Cl}]$, 1.980 Å. A similar trend was observed in all “[ML_2]” complexes [$\text{M} = \text{Fe}(\text{III})$, $\text{Co}(\text{III})$, $\text{Ni}(\text{II})$, and $\text{Ni}(\text{IV})$].³

Absorption Spectra. The absorption spectral studies are the easiest means of characterization of ruthenium(III) complex **1** as well as its oxidized counterpart **2**. As was observed for other complexes of $\text{L}(2-)$, in the visible region the absorption spectrum of complex **1** is dominated by ligand-to-metal charge-transfer (LMCT) transitions. In MeCN/ CH_2Cl_2 solution, an intense absorption at ~ 440 nm justifies its color. Oxidized product **2** is clearly identifiable by its characteristic strong absorption feature at ~ 650 nm, with enhancement in extinction coefficients compared to its ruthenium(III) counterpart. A similar trend was observed before.^{6b} The absorption spectra of **1** and **2** in CH_2Cl_2 are displayed in Figure 2. It is worth noting here that the strongly allowed LMCT band at 386 nm for activated iron(III) bleomycins, which has a deprotonated amide coordination, was shown to be a deprotonated amide-to-iron π -LMCT band; the weakly allowed transition originating from a delocalized pyrimidine/amide σ -orbital occurs at somewhat lower energy.²¹ We believe that for **1** this transition is observed at ~ 440 nm.

EPR Spectra. The EPR spectra of low-spin ruthenium(III) complex **1** were recorded as a microcrystalline solid and in MeCN solution, at 300 K and at 77 K, and also as a glass in MeCN–toluene (1:1.2 v/v) to probe the electronic ground state and distortion parameters. For **1**, in the polycrystalline state the spectral parameters are 2.221 and 1.924 (300 K); 2.204 and 1.917 (77 K). In MeCN solution, the signal is isotropic: 2.116 (300 K) and 2.168 (77 K). In MeCN–toluene glass (1:1.2 v/v) the signal is also isotropic (2.168). Thus, in the solid state the spectral data show axial symmetry with two principal g values. It should be noted here that the

(19) Dutta, S.; Bhattacharya, P. K.; Tiekink, E. R. T. *Polyhedron* **2001**, *20*, 2027.

(20) Ko, P.-H.; Chen, T.-Y.; Zhu, J.; Cheng, K.-F.; Peng, S.-M.; Che, C.-M. *J. Chem. Soc., Dalton Trans.* **1995**, 2215.

(21) Neese, F.; Zaleski, J. M.; Zaleski, K. L.; Solomon, E. I. *J. Am. Chem. Soc.* **2000**, *122*, 11703 and references therein.

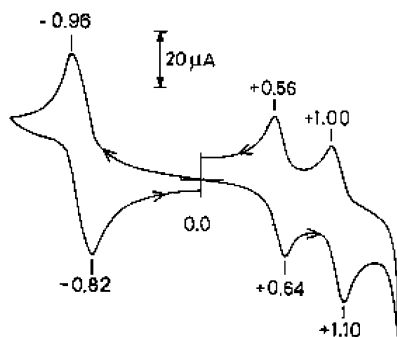


Figure 3. Cyclic voltammogram (100 mV/s) of a 1.02 mM solution of $[\text{Et}_4\text{N}][\text{RuL}_2]\cdot\text{H}_2\text{O}$ (**1**) at a platinum electrode in CH_2Cl_2 (0.2 M in TBAP). Indicated potentials (in V) are vs SCE.

X-ray results have shown that the Ru atom in complex **1** has tetragonally compressed octahedral geometry and therefore is revealed by its axial EPR spectra (Figure S2, Supporting Information). We have analyzed the g values obtained in the polycrystalline state at 77 K according to the well established theory for the low-spin d^5 system.^{21,22} The distortion in **1** can be quantitated with the help of the experimental g values and the \mathbf{g} tensor theory of low-spin d^5 complexes. Details of the methods used by us can be found elsewhere.^{6a,22} The axial splitting parameter (Δ , expressed in terms of spin-orbit coupling constant λ) is 6.025. Taking $\lambda \sim 1000 \text{ cm}^{-1}$,²² the energies of the crystal field transitions (ΔE_1 and ΔE_2) are predicted to be $\sim 5700 \text{ cm}^{-1}$ ($\sim 1750 \text{ nm}$) and $\sim 6600 \text{ cm}^{-1}$ ($\sim 1500 \text{ nm}$). A relatively weak and broad band is indeed observed in MeCN solution of **1** at 1400 nm (Figure 2). The spectral result thus demonstrates that the ground state of complex **1** is correctly represented by the chosen solution.

Redox Properties. To investigate the extent of stabilization of the ruthenium(III) state toward reduction and whether a possibility corresponding to the accessibility of higher oxidation states could be achieved, cyclic voltammetric (CV) studies on **1** were performed. CV studies on **2** were performed to examine whether it is the one-electron oxidized form of **1**.

(a) Metal Reduction of Ruthenium(III) Complex. The CV scan of **1** in MeCN at a platinum working electrode shows (Figure S3, Supporting Information) a reversible^{11b} reductive response at $E_{1/2}$ of -0.84 V vs SCE ($\Delta E_p = 80 \text{ mV}$) due to $\text{Ru}^{\text{III}}-\text{Ru}^{\text{II}}$ redox process. The one-electron nature of this redox response has been confirmed by (i) comparison of current height with the redox response of samples of $[\text{M}^{\text{III}}\text{L}_2]^-$ ($\text{M} = \text{Fe}, \text{Co}, \text{and Ni}$), $[\text{Ni}^{\text{III}}\text{L}_2]^{2-}$, or $[\text{Ni}^{\text{IV}}\text{L}_2]$ species, under the same experimental conditions, as well as by constant-potential electrolysis (see details in a following paragraph). The CV scan of **1** in CH_2Cl_2 ²³ [$E_{1/2}$ of -0.89 V vs SCE ($\Delta E_p = 140 \text{ mV}$)] is displayed in Figure 3. The observed stabilizing potential of $\text{L}(2-)$ toward the Ru(III) state must be due to the presence of four deprotonated amide

nitrogen species coordinating. In fact, the $E_{1/2}$ values (V vs SCE) for the $\text{M}^{\text{III}}-\text{M}^{\text{II}}$ couple follow the following trend: $\text{Co} (-1.10) < \text{Fe} (-0.91) < \text{Ru} (-0.84) < \text{Ni} (0.05)$.³ Thus, the Fe(III) state is better stabilized than the Ru(III) state by $\text{L}(2-)$ in their bis-ligand complexes. A trend in a similar direction was found for $\text{M}(\text{terpy})_3^{3+}/\text{M}(\text{terpy})_3^{2+}$ ($\text{terpy} = 2,2':6',2''\text{-terpyridine}$; $\text{M} = \text{Fe}$ or Ru ; $E_{1/2}$ (V vs SSCE) = 1.09 for Fe and 1.27 for Ru) redox processes in MeCN.²⁴ In both systems, the spin-state properties of bivalent and trivalent species are expected to remain invariant, due to the strong field nature of the ligands.

(b) Oxidative Response of Ruthenium(III) Complex. When scanned anodically, complex **1** displays in MeCN solution two reversible one-electron oxidative responses at $E_{1/2}$ of 0.59 V ($\Delta E_p = 60 \text{ mV}$) and 1.05 V ($\Delta E_p = 100 \text{ mV}$) versus SCE (Figure S3, Supporting Information). The anodic CV scan of **1** in CH_2Cl_2 (Figure 3) displays two responses at $E_{1/2}$ of 0.60 V ($\Delta E_p = 80 \text{ mV}$) and 1.05 V ($\Delta E_p = 100 \text{ mV}$) versus SCE. These couples are of considerable interest with regard to the oxidation state of ruthenium. For the less positive oxidative response, two alternative formal descriptions are possible: (1) It is a $\text{Ru}^{\text{IV}}-\text{Ru}^{\text{III}}$ couple, and therefore, in the oxidized complex **2** ruthenium is present in the tetravalent state. (2) It is a ligand-centered oxidative response, and hence, complex **2** is a ruthenium(III)-stabilized ligand π -cation radical complex. Admittedly, few genuine homoleptic complexes of ruthenium(IV) are known, and those reported invariably have strongly σ -donating anionic ligands. To our knowledge, among pyridine amide complexes of trivalent metal ions, barring that observed for $[\text{FeL}_2]^-$ and $[\text{CoL}_2]^-$ complexes, no examples of the latter description exist in the literature. As we have shown (vide infra), the observed redox responses are due to ligand-centered oxidations.

On the basis of the electronic structural analysis on activated bleomycins by Solomon et al.,²¹ we are inclined to believe that highest energy ligand-based orbitals are localized on the deprotonated amide moiety.

(c) Redox Processes of Isolated Oxidized Complex. The CV scan of **2** in CH_2Cl_2 (Figure S4, Supporting Information) displays two reductive responses: $E_{1/2} = -0.88 \text{ V}$ versus SCE ($\Delta E_p = 120 \text{ mV}$) and $E_{1/2} = 0.59 \text{ V}$ ($\Delta E_p = 100 \text{ mV}$) versus SCE. Thus, identical behavior to that observed for complex **1** is observed, excluding the more positive response at 1.05 V versus SCE. One-electron nature of the responses of **2** has been confirmed by coulometric experiments [applied potential, 0.2 V, n (the number of electrons passed per molecule) = 0.98; applied potential, -1.0 V , $n = 1.12$]. The clean nature of the cyclic behavior of **2** documents the purity and authenticity of the isolated one-electron chemically (Ce^{4+}) oxidized form of **1**. The reductive response at 0.59 V is due to $[\text{RuL}_2]^{0/-}$ redox process (reduction of cation radical), and the redox process at -0.88 V is due to $[\text{RuL}_2]^{1-/2-}$ (metal-centered reduction).

In an attempt to provide proof of the existence of the proposed ligand cation, coulometric one-electron oxidation

(22) (a) Bhattacharya, S.; Ghosh, P.; Chakravorty, A. *Inorg. Chem.* **1985**, *24*, 3224 and references therein. (b) Taqui Khan, M. M.; Srinivas, D.; Kureshy, R. I.; Khan, N. H. *Inorg. Chem.* **1990**, *29*, 2320 and references therein.

(23) Under our experimental conditions, the $E_{1/2}$ values (V) for couple Fc^+/Fc were 0.40 (MeCN) and 0.49 (CH_2Cl_2) vs SCE.

(24) Morris, D. E.; Hanck, K. W.; DeArmond, M. K. *J. Electroanal. Chem.* **1983**, *149*, 115.

of green $[\text{Et}_4\text{N}][\text{CoL}_2]\cdot 2\text{H}_2\text{O}$ to generate “[CoL_2]” at 1.2 V versus SCE was attempted. However, it should be noted here that even on the CV time-scale the oxidation peak profile, supposedly due to formation of ligand cation,^{3a} is not ideally suited to generate electrochemically a stable ligand cation species. The electrochemically generated transient solution species (color changes from green to brownish green) very quickly (within 10–15 s) decomposes/changes to another species (yellow). Unlike $[\text{Et}_4\text{N}][\text{CoL}_2]\cdot 2\text{H}_2\text{O}$, this yellow solution did not exhibit a well behaved CV response. Either brownish green (this solution changes its color instantaneously to yellow even at 77 K) or yellow solutions did not display any EPR signal. Given the results at hand, we are not in a position to provide spectroscopic proof of the existence of the proposed radical cation from EPR spectroscopy on “[CoL_2]”. Efforts are on to throw more light on the nature of ligand oxidation process(es) in (i) $[\text{RuL}_2]^-$, (ii) $[\text{FeL}_2]^-$, and (iii) $[\text{CoL}_2]^-$ (with suitably ring substituted variety of $\text{L}(2-)$), the results of which will be published elsewhere.

Magnetism. (a) $[\text{Et}_4\text{N}][\text{RuL}_2]\cdot \text{H}_2\text{O}$. The magnetism of complex **1** was investigated over the temperature range 81–300 K (Faraday magnetometer) to define spin-state and allow structural inferences. It follows the Curie–Weiss law (Figure S5, Supporting Information), which is typical for low-spin six-coordinate ruthenium(III) complexes. Due to large spin–orbit coupling, the observed μ_{eff} values ($2.20 \mu_{\text{B}}$ at 300 K and $1.58 \mu_{\text{B}}$ at 81 K) are larger than the spin-only value of $1.73 \mu_{\text{B}}$. Thus, the observed result clearly demonstrates the $S = 1/2$ ground state of **1**, which is in excellent agreement with the X-band EPR spectral behavior of a powdered sample of **1** (see a following paragraph). The effective magnetic moment of **1** in MeCN solution is $2.14 \mu_{\text{B}}$ (300 K), in good agreement with the solid-state value.

(b) $[\text{RuL}_2]\cdot \text{H}_2\text{O}$. Because we were unable to grow single crystals for compound **2**, structural information is lacking. An attempt was made to choose between the two alternative descriptions of the electronic structure of **2** (vide supra) by using temperature-dependent (54–300 K) magnetic susceptibility studies. The μ_{eff} value at 300 K ($1.03 \mu_{\text{B}}$) reveals the quenching of the unpaired spins, in sharp contrast to that of **1**. If it were a ruthenium(IV) complex, then at room temperature, the μ_{eff} value would have been in the range 2.7–2.9 μ_{B} , as observed for an authentic six-coordinate ruthenium(IV) complex (it is a d^4 system and therefore is expected to show paramagnetism corresponding to two unpaired electrons) of a tetradentate salicylamide ligand.²⁵ The observed μ_{eff} value points toward the ligand cation radical description. The $\chi_{\text{M}}T$ value monotonically decreases with a lowering of the temperature ($\chi_{\text{M}}T = 0.135 \text{ cm}^3 \text{ mol}^{-1} \text{ K}$ at 300 K and $\chi_{\text{M}}T = 0.026 \text{ cm}^3 \text{ mol}^{-1} \text{ K}$ at 54 K) (Figure S6, Supporting Information), which is suggestive of the existence of strong antiferromagnetic coupling. The unpaired electron spin of a ligand π -cation radical (see above) couples invariably intramolecularly and strongly to the unpaired

electron spin of an incompletely filled t_{2g} subshell of Ru(III), rendering complex **2** diamagnetic at 300 K.

In CDCl_3 solution, complex **2** displays a clean ^1H NMR spectrum (Figure S7, Supporting Information), closely similar to that observed for $[\text{Co}^{\text{III}}\text{L}_2]^-$ and $[\text{Ni}^{\text{IV}}\text{L}_2]$,³ attesting to its diamagnetic ground state. Assignment of the signals (Experimental Section) has been made through consideration of relative peak areas and comparison with free ligand spectra.

Summary and Conclusions. The following are the principal findings and conclusions of this investigation. (1) We have succeeded in synthesizing a new bis-ligand ruthenium(III) complex of meridionally coordinated tridentate pyridine amide $\text{L}(2-)$ ligand. Structural characterization has revealed that the metal ion is coordinated in tetragonally compressed geometry with four nonmacrocyclic tetradentate N-coordination in the equatorial plane and two axial pyridine coordination. To the best of our knowledge, this is the first time that a ruthenium(III) complex coordinated solely by two tridentate deprotonated peptide ligands has been synthesized and structurally characterized. (2) Redox properties of **1** unravel the attainment of a highly stabilized ruthenium(III) state (Ru^{III}/Ru^{II} redox process) and a ligand-centered oxidative response. (3) We have shown in this study that dipeptide ligand $\text{L}(2-)$ is a noninnocent ligand in the sense that it can exist in two different oxidation levels in coordination compounds: (i) dianion and (ii) monoanion (ligand π -radical). The data reported herein indicate that by using the dianionic dipeptide ligand having picolinamide functionality stable π -radical cation complexes of low-spin ruthenium(III) can be isolated in analytically pure form for detailed characterization. To the best of our knowledge, this report documents the first example of such a complex with a tridentate pyridine amide ligand system. The stabilization of a π -radical cation form of $\text{L}(2-)$ is achieved by an intramolecular antiferromagnetic coupling with a low-spin ruthenium(III) center with incompletely filled t_{2g} subshell. The latter description has as yet not been structurally characterized in a complex, but electronic structure of **2** has been established to a reasonable level of confidence.

Acknowledgment. This work is supported by grants from the Council of Scientific and Industrial Research and Department of Science and Technology, Government of India, New Delhi. We sincerely thank Prof. Samaresh Bhattacharya, Jadavpur University, Kolkata, India for his help with low-energy absorption spectral measurements on **1**. Constructive comments of reviewers were very helpful at the revision stage.

Supporting Information Available: IR spectra of **1** and **2** (Figure S1), EPR spectrum of **1** in MeCN–toluene glass (Figure S2), CV scan of **1** in MeCN (Figure S3) and **2** in CH_2Cl_2 (Figure S4), plot of molar magnetic susceptibility vs temperature for **1** (Figure S5) and plot of $\chi_{\text{M}}T$ versus T for **2** (Figure S6), and ^1H NMR spectrum of **2** in CDCl_3 at 300 K (Figure S7). Crystallographic data in CIF format. This material is available free of charge via the Internet at <http://pubs.acs.org>.

(25) Che, C.-M.; Cheng, W.-K.; Leung, W.-H.; Mak, T. C. W. *J. Chem. Soc., Chem. Commun.* **1987**, 418.